ISSN 1330-3651 (Print), ISSN 1848-6339 (Online)
https://doi.org/10.17559/TV-20230614000736
Preliminary communication

Analytical, Numerical and Experimental Performance Prediction of a Model-Sized Wind Turbine

Matej FIKE*, Andrej PREDIN, Gorazd HREN, Marko PEZDEVŠEK

Abstract: The present work focuses on the comparison of the capabilities of Blade Element Momentum Theory, with and without the high induction factor value model and Computational Fluid Dynamics modelling in relation to experimental measurements of the power coefficient for a model-sized horizontal axial wind turbine. Initially, an analytical investigation was performed to obtain the power coefficient curve. Furthermore, three-dimensional numerical simulations were performed, where a lot of effort was devoted to the preparation of a low *y+* structured mesh. Analytical and numerical results of the power coefficient were compared with experimental results, which were obtained with our own conducted experiments in the wind tunnel. The most significant conclusions are that the classic BEM method deviates from measured data in the entire range of tip speed ratios, the BEM method with Spera correction predicts a significantly better agreement with experimental measurements compared to the classic BEM method, especially the part where the power coefficient decreases and finally that CFD computations can accurately predict the performance of wind turbines and compute the flow around an aerofoil of the blade.

Keywords: BEM Method; CFD; measurements; wind turbine

1 INTRODUCTION

To reduce climate change and environmental degradation, the European Green Deal (EGD) is a new strategy to transform the European Union (EU) into an efficient and competitive economy with resources. The EGD goal is to make Europe climate neutral by 2050, enhance green technologies and cut pollution. Europe already has a substantial record in reducing its greenhouse gas emissions while maintaining economic growth. Decarbonising the energy system is critical to achieve the EU's climate objectives in 2050, while energy needs to be available and affordable for consumers and businesses. Europe has to transform its energy systems into an integrated and competitive Europe energy market that is based mostly on renewable sources and promotes high investments in green energy and energy efficiency.

Wind energy is close to ideal to be the EGD's choice technology to help the EU economy: it is cost-competitive and it is scalable. The wind technology already represents 15% of Europe's source of electricity. Europe needs to scale-up wind energy production in order to keep global warming below 2 degrees Celsius and deliver on its Paris Climate Agreement commitments. According to the European Commission's Long-Term Decarbonisation Strategy, Europe will need between 700 and 1200 GW of wind capacity up from today's 190 GW [1].

The performance of wind turbines can generally be analysed in three ways, analytically, numerically, and experimentally. The analytical approach is usually the use of the BEM method, the numerical approach is the use of computational fluid dynamics and the experimental approach is the physical measurement of usually model-sized wind turbines in wind tunnels.

All three approaches were used in the study conducted by Lee et al. [2]. They were investigating the power performance of a horizontal axis wind turbine (HAWT) with two different types of blades. Hasan et al. [3] present a study between the analytical BEM method and CFD analysis of a HAWT. They showed that the performance of wind turbine blades by CFD computation is a little bit less than by BEM. The reason behind the discrepancy is that the CFD method can more accurately predict 3D effects comparative to BEM. The same conclusion was reached in a study done by Dimitriadis et al. [4]. In the work of Rodriguez et al. [5] a comprehensive methodology for wind turbine blade optimization was proposed using CFD and BEM methods.

Muhsen et al. [6] were designing a small wind turbine by employing BEM theory and optimizing its performance using the software QBlade. Khaled et al. [7] dealt with aerodynamic design and blade angle analysis of a small wind turbine. They used an in-house program based on BEM theory and CFD for analysis of HAWT blade cross-section at various blade angles. In [8] the effect of turbulence on the power performance at the yawed and no-yawed flow conditions was investigated. The authors focused on turbulence intensities and boundary layer in wind tunnel experiments. They found out the power coefficient decreased in the case of extremely low turbulence intensity. Hren [9] performed a numerical analysis of a wind turbine blade with different software using Ansys CFX and SolidWorks. He found that plug-in software is still inadequate for nontrivial problems. The parametric and numerical optimisation of aerofoil profiles by CFD was performed by [10] looking for the maximum power coefficient by changing solidity. Haghighi et al. [11] wrote a paper presenting a comprehensive review of progress on optimization of wind turbine performance using CFD, illustrating the functions to determine the performance of a wind turbine.

Full three-dimensional calculations are still very time-consuming and expensive and can take considerable time, especially for preliminary design, optimization of blade shape, and overall optimization of wind turbines. This paper compares the accuracy of BEM and CFD with experimental measurements. CFD can include more physics that is neglected in BEM and therefore has higher accuracy.

2 BLADE GEOMETRY

The horizontal axes wind turbine examined in this paper has been developed for testing in the Laboratory for

Aero and Hydro Energy Technology, which is a part of the Institute of Energy Technology at the University of Maribor. To perform 3D printing and CFD modelling, the geometry needs to be exactly described in a digitised format. Wind turbine blades have complex geometry with varied twist angles and chord lengths at span-wise cross-sections from hub to tip. The wind turbine consists of three blades. The initial shape of the blade was taken from [12] with a tip radius of 0,45 m and an S826 aerofoil. The blade was divided into 28 sections along the span-wise direction from the hub to the tip. The lower four cross-sections were adapted to create a smooth transition for the blade attachment. The in-house application was used to scale and rotate aerofoil profiles according to their center of gravity to get coordinates of each span-wise section. Macro-program was used to generate a solid body of the blade in SolidWorks 2020. Due to the 3D printer height limitation, the original blade was scaled by a factor of 0,74. A new blade hub was also modelled. The diameter of the rotor was 0,63 m. The modelled blade and some cross-sections used are shown in Fig. 1.

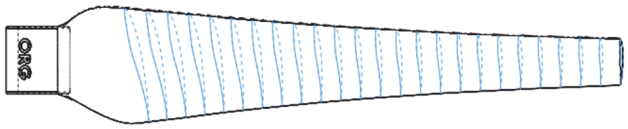

Figure 1 Wind turbine blade

3 BEM METHOD

BEM theory is based on two decompositions, a radial decomposition of the blades and the fluid column, considered as concentric rings that do not interact with each other, and a decomposition of the fluid/turbine system into a visible part via Momentum Theory and a local planar part via Blade Element Theory [13].

Momentum-theory deals with forces that produce fluid motion by the rotating blades. The blade element theory is related to the forces on the blades due to the fluid flow. By this method, the wind turbine blade is divided into smaller cross-sections segments along the blade. Consequently, the conservation of one-dimensional linear momentum is applied to each segment of the blade followed by forces and power calculations. In the BEM method, there are two main key issues, the induction factor, and aerofoil aerodynamic characteristics. The calculations were performed by in-house software written in Python that was used to predict the power characteristics of wind turbines. In our case, the entire blade was divided into 28 segments for BEM analysis. In the iterative process of BEM, for every segment of the blade, the lift and drag coefficients were calculated until convergence with induction factors was reached. Several high values of axial induction factor correction models were applied in BEM. In this paper only results from classic BEM theory without any correction models and with Spera [14] correction model will be presented and discussed. Other correction models such as tip and hub losses, cascade correction, skew wake correction, and rotational augmentation correction were not considered.

4 NUMERICAL SIMULATIONS

CFD has received great attention in recent years, as it is a promising tool for simulating the flow around wind turbine blades and visualising flow fields as well as predicting wind turbine efficiency. The geometry of the wind turbine blade together with the computational domain was prepared in SolidWorks. A domain is a space with various limitations and initial conditions in which a fluid, in this case, air, will flow at a prescribed speed. Air flows on each blade of a wind turbine with the same velocity profile, so it is assumed that the conditions on each blade are the same. Due to the reduction of the number of elements and consequently calculation time, the condition of rotational periodicity was given, and only one-third of the cylinder volume was taken into account. The obtained result is multiplied by the number of blades and thus we get the same result as if we simulated the entire wind turbine. The periodicity condition in its calculation equations already takes into account the 3D effects on the blade and the flow around it, which in reality arise due to the influence of the previous blade on the next one. The geometry of wind blade together with calculation domain was prepared in SolidWorks 2020. The size of the numerical domain was 10 blade lengths upstream and 20 blade lengths downstream.

4.1 Mesh

Meshing is a crucial part of performing numerical simulations and has an important impact on the accuracy of numerical results and computational time. It is challenging to prepare a quality mesh for CFD modelling of wind turbines. The most appropriate mesh for simulating wind turbine performance is a structured mesh. In a structured mesh, grid connections are regular and abutting elements are in particular order. It has advantages in low memory usage, better convergence, and high resolution of geometry but on the other hand, it is time-consuming and hard to generate due to the complex geometry of wind turbine blades where the ratio between chord length and span-wise domain length is significantly larger at the hub compared to the tip.

Due to a reduction of the number of elements and consequently calculation time, the condition of rotational periodicity was used and only one-third of the cylinder volume described by the wind turbine was taken into account. The obtained numerical result is multiplied by the number of blades and thus we get the same result as if we simulated the entire wind turbine. The periodicity condition in its calculation equations already takes into account the 3D effects on the blade and the flow around it, which in reality arise due to the influence of the previous blade on the next one.

When creating a structured mesh, it was necessary to mark and name the surfaces on the domain. With this, we prepared and facilitated our work in advance, as it was subsequently much easier to determine the boundary conditions of the corresponding surfaces.

This was followed by dividing the domain into sections. With this operation, we achieved as good a mesh distribution as possible via geometry. It was necessary to associate the edges of the sections to the curves of the vane

geometry, thereby determining where the numerical grid should extend. It was then necessary to set the desired number of elements on each of the sections while paying attention to the aspect ratio between the size of the elements near and far from the blade, the transition between the sizes of the elements of different sections, the smallest angles of the elements and the total number of elements. In theory, we have two approaches to Reynolds averaged Navier-Stokes simulation (RANS), a low $y+$ simulation or a high $y+$ one. This corresponds to the non-dimensional height of the first layer closest to the wall. We used a low $y+$ approach, where the entire laminar sublayer is calculated. The generated mesh has small elements right next to the blade, with small $y+$ values, where we have a large velocity gradient and larger elements in front of the blade. In this part, the shape of the flow is known. In Fig. 2 and Fig. 3 the mesh at the height r/R = 0,33 and r/R = 1 is shown, respectively.

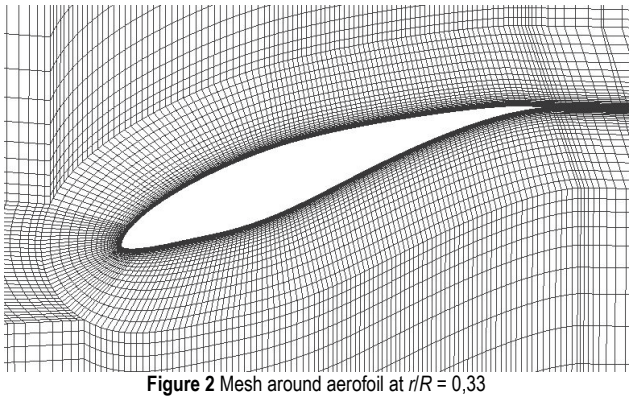

Figure 2 Mesh around aerofoil at r/R = 0,33

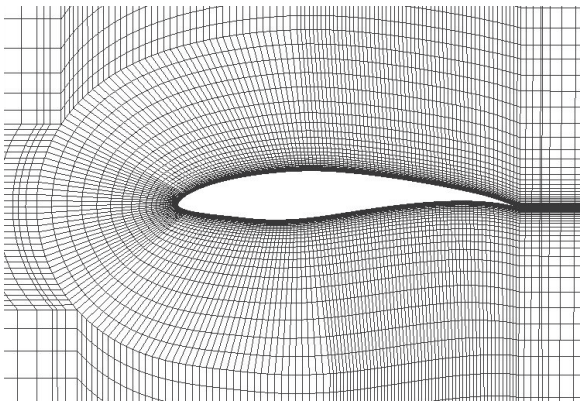

Figure 3 Mesh around aerofoil at r/R = 1

The final mesh had 11256682 elements; the quality is shown in Fig. 4. The mesh quality factor determinant calculates the deformation of each cube in the mesh based on the Jacobi determinant and then normalizes the matrix determinant. A value of 1 represents a perfect cube while a value of 0 represents a deformed cube with negative volume. In general, mesh quality values above 0,3 are acceptable for most solvers.

The generated computational meshes ranged from 11 to 20 million hexahedral elements, refined both horizontally and radially. To evaluate the grid independence and to calculate the CGI, we monitored the coefficient of power at a tip speed ratio of 5.8 on three hexa-structured meshes, generated using ANSYS-ICEMCFD. Following the results of this analysis, the discretization uncertainty was calculated. The grid convergence index presenting the calculated uncertainty was less than 1% for fine mesh and also less than 1% for medium mesh. To assure minimal computational time, the initial mesh was used for further analysis.

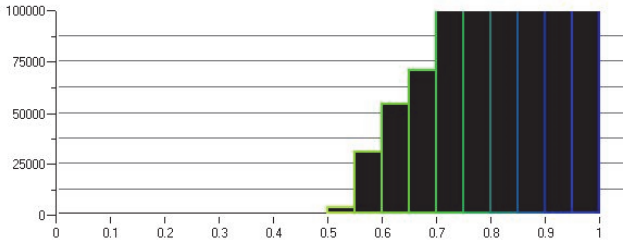

Figure 4 Mesh quality

4.2 Boundary Conditions

Steady-state simulations were performed with ANSYS 2020 CFX. The prescribed boundary conditions and computational domain are shown in Fig. 5. At the inlet surface, the Velocity Inlet was given as a boundary condition and a velocity of 5,2 m/s was prescribed. On the other side of the domain, at the outlet surface, the Pressure Outlet boundary condition was used, where a relative static pressure of 0 Pa was set. The left and right surfaces were defined as rotational periodicity. At the hub and shroud surfaces, free slip wall boundary condition was set. The blade surface was defined as a rotating no-slip wall.

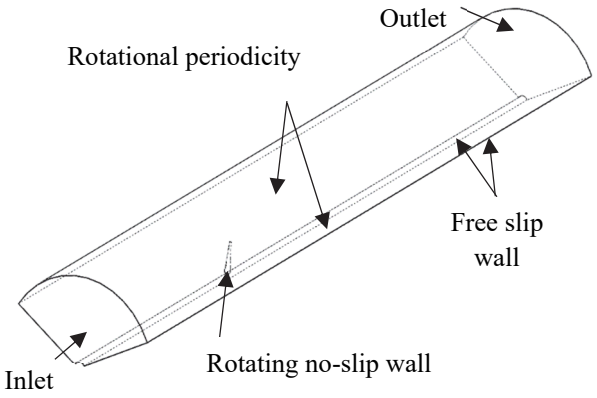

Figure 5 Computational domain and boundary conditions

In the analysis the air density of 1,225 kg/m³ and dynamic viscosity of $1{,}79 \times 10^{-5}$ kg/(m s) were prescribed for incompressible fluid with isothermal conditions. Reynolds averaged Navier-Stokes models provide approximate time-averaged solutions to the Navier-Stokes equations, focusing on non-fluctuating and large-scale features of the flow. For two-equation RANS turbulence models, the k-ε and k-ω models are widely used in the CFD modelling of wind turbines. k-ω turbulence model involves the solution of transport equations for the turbulence kinetic energy (k) and the specific rate of dissipation (ω). The most frequently used variant of the k-ω turbulence model is the k-ω Shear Stress Transport model (SST), which results match well with experimental results [15]. For this reason, the SST turbulence model was used in our simulations. We inserted equations into the simulation's monitor points to calculate and monitor the blade torque

and power coefficient. With this, we checked whether the calculated variables had stabilized and whether the convergence criterion was reached.

5 EXPERIMENTAL SETUP

Wind turbine power coefficient characteristics were measured in a closed-loop wind tunnel. The wind tunnel has a test cross-section of 2 m × 2 m and is powered by a 160 kW fan. Measurements were performed at the wind speed of 5,2 m/s. Inflow velocity was determined with 2D LDA system 2D FLX 500 FlowExplorer placed on a lightweight traverse system. The wind turbine rotor was attached to the electromotor and regulated with a frequency converter to control the rotational speed of the wind turbine. The electric motor was floating attached to a stand. A lever was attached to the motor housing, which prevented rotation around its axis via force sensor HBM U9C 200N as shown in Fig. 6. Measurements were done with varying rotational speeds of the wind turbine, keeping all other parameters constant. The largest uncertainty of the power coefficient measurements may be taken as 10%, especially in the wind turbine operating conditions where the local angle of attack is increasing over the blade indicating that the dynamic effects are related to flow separation.

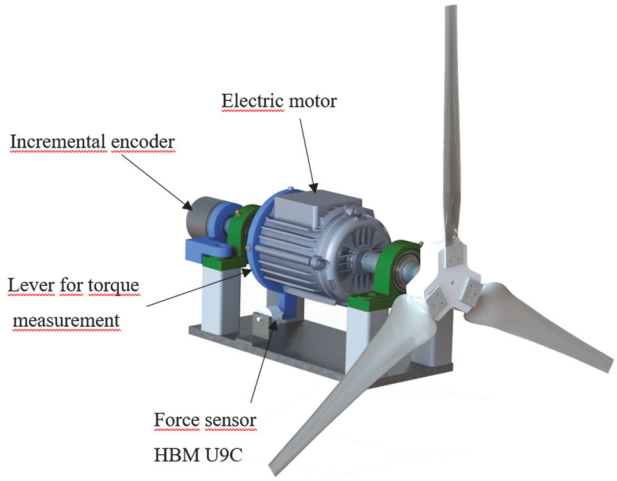

Figure 6 A small scaled wind turbine connected to electromotor

6 RESULTS AND DISCUSSION

6.1 Power Coefficient

Fig. 7 compares the power curve obtained by the classic BEM, CFD with the experimental measurements against different tip speed ratios (*TSR*). The figure shows a good agreement between CFD results and the experimental data and a poor agreement between the classic BEM method and experimental data. Considering the first part, where the tip speed ratio is smaller than 5, the predicted curve of the classic BEM method deviated from the measured one. In the second part ($5 < TSR < 10$), the predicted power coefficient is less than the measured data. Almost in the entire observed range, it is possible to observe a good agreement of the course of the power coefficient between the CFD values and the measured values. A small deviation can be observed at the value of 3,5 and in the region where CFD predicts higher values of the power coefficient compared to the measured values. The highest power coefficient in the classic BEM method is 0,444, in the CFD method 0,454 and the measured value is 0,448. The values of the maximum efficiency are very close, but we can notice the difference in the location of the maximum value, or at which value of *TSR* the maximum of the power coefficient is reached. The classic BEM method predicts the power coefficient peak at *TSR* 5, the CFD method at 6,1, and the highest measured value is at 5,8. The classic BEM method deviates from experimental data in the entire range of tip speed ratios. The Spera correction for high induction factor values was used and results are shown in Fig. 7. Comparing the classic BEM and Spera, the whole diagram can be divided into two parts. The first part shows an excellent agreement between both BEM methods. In the second part, the results differ. The BEM method with Spera correction predicts a significantly better agreement with experimental measurements compared to the classic BEM method.

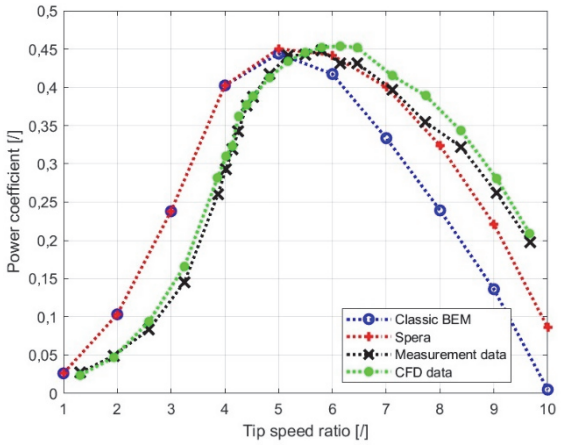

Figure 7 Power coefficient versus tip speed ratio between Classic BEM, Spera BEM, CFD and measurements

The predicted and measured power coefficients were compared with the coefficient of determination and calculated values are shown in Tab. 1.

Table 1 Calculated coefficient of determination

Method	R^2
Classic BEM	0,6395
Spera BEM	0,8191
CFD	0,9928

The calculation of the coefficient of determination shows that the best method is the CFD method, followed by Spera and Classic BEM.

One of the reasons for the difference between the BEM method and the CFD method is using 2D lift and drag coefficients. Although the Spera correction for high induction factor values was used, the CFD results provided also visualizations of the flow through the turbine and around blades to get a complete idea about performance. In CFD the predetermined aerodynamic data, like lift and drag coefficients, was not used to calculate the performance.

The errors associated with the BEM can be attributed to the angles of attack which are different due to the complex nature of the three-dimensional flows [16]. The three-dimensional flow changes axial and rotational induction factors; consequently the relative flow angle and magnitude alter. Errors in the prediction of the lift and drag

forces result in errors in power prediction. Complete accurate CFD modeling is necessary to determine the wind turbine performance. However, the BEM method with various correction models is a good starting point for power coefficient predictions.

6.2 Flow Around an Aerofoil

Fig. 8 and Fig. 9 present flow around an aerofoil of the wind turbine blade at two different spanwise locations, r/R = 0,25 and r/R = 0,9; respectively. It is evident when looking at these two figures, the blade seems to be fully stalled at very low tip speed ratios, with separation from the leading to the trailing edge of the blade.

The velocity gradient at the surface is zero when separation occures and consequently the viscous friction force has to be zero. Separation occurs on the downwind side of bodies in fluid flow, causes high form drag for unsharp bodies and stalled aerofoils. In the separation zone, the velocities are low or even of negative values. Therefore the boundary layer grows, producing an increase of the displacement thickness. This alters the effective geometry of the airfoil, which is reflected in reducing its aerodynamic performance. As the number of tip speed ratio decreases, the angle of attack of an aerofoil increases, and the separation points move toward the leading edge.

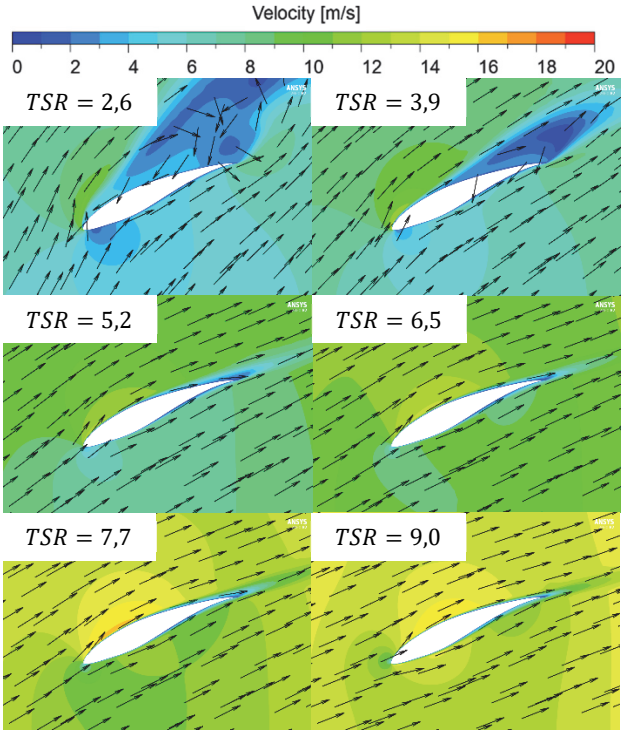

Figure 8 Flow around aerofoil at r/R = 0,25 at various tip speed ratios

At TSR = 3,9; about three-quarters of aerofoil in the entire span from the hub to the tip are stalled. As the TSR increases beyond the optimal value, Fig. 8 and Fig. 9 show that the angle of attack decreases, which is reflected in a decrease in the lift force and, consequently, in a deterioration of the performance.

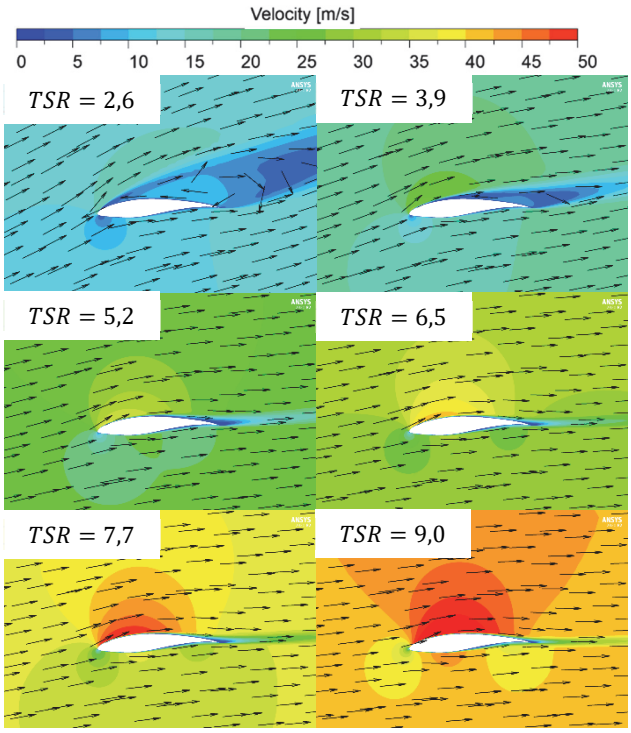

Figure 9 Flow around aerofoil at r/R = 0,9 at various tip speed ratios

The three dimensional effects present for low tip speed ratios need further examination of the relevant forces acting on the blade. The effects are caused by large spanwise variations in the force distribution on the blade combined with rotational augmentation.

7 CONCLUSION

In this study, the performance of a model-size horizontal wind turbine was fully investigated analytically, numerically, and experimentally. In-house software based on BEM theory was used. Classic BEM method and Spera correction for high induction factor values were used for power coefficient calculation. Numerical simulations were implemented to predict the performance of a wind turbine and to analyse the flow around wind turbine blades. A low $y+$ approach and low-Reynolds model was used. Power coefficient results from an in-house software and CFD were compared with measurements performed in a closed loop wind tunnel.

The most significant conclusions are that the classic BEM method deviates from measured data in the entire range of tip speed ratios. The BEM method with Spera correction predicts a significantly better agreement with experimental measurements compared to the classic BEM method, especially the part where the power coefficient decreases and finally that CFD computations can accurately predict the performance of wind turbines and compute the flow around an aerofoil of the blade.

8 REFERENCES

[1] https://windeurope.org/about-wind/campaigns/european-green-deal/ {1.6.2023}

[2] Lee, M. H., Shiah, Y. C., & Bai, C. J. (2016). Experiments and numerical simulations of the rotor-blade performance for a small-scale horizontal axis wind turbine. *Journal of Wind Engineering and Industrial Aerodynamics*, *149*, 17-29.

https://doi.org/10.1016/j.jweia.2015.12.002
[3] Hasan, M., El-Shahat, A., & Rahman, M. (2017). Performance Investigation of Three Combined Airfoils Bladed Small Scale Horizontal Axis wind Turbine by BEM and CFD Analysis. *Journal of Power and Energy Engineering*, *05*(05), 14-27. https://doi.org/10.4236/jpee.2017.55002
[4] Martinopoulos, G. & Missirlis, D. (2014). Investigation of the Performance of a Horizontal Axis Wind Turbine With the Use of Blade Element Momentum Theory and Cfd Computations. *Conference: European Wind Energy Association 2014*, Barcelona
[5] Rodriguez, C. V. & Celis, C. (2022). Design optimization methodology of small horizontal axis wind turbine blades using a hybrid CFD/BEM/GA approach. *Journal of the Brazilian Society of Mechanical Sciences and Engineering*, *44*(6), 1-25. https://doi.org/10.1007/s40430-022-03561-4
[6] Muhsen, H., Al-Kouz, W., & Khan, W. (2020). Small wind turbine blade design and optimization. *Symmetry*, *12*(1). https://doi.org/10.3390/sym12010018
[7] Khaled, M. (2017). Aerodynamic Design and Blade Angle Analysis of a Small Horizontal Axis Wind Turbine. *American Journal of Modern Energy*, *3*(2), 23. https://doi.org/10.11648/j.ajme.20170302.12
[8] Li, Q., Kamada, Y., Maeda, T., Murata, J., & Yusuke, N. (2016). Effect of turbulence on power performance of a Horizontal Axis Wind Turbine in yawed and no-yawed flow conditions. *Energy*, *109*, 703-711. https://doi.org/10.1016/j.energy.2016.05.078
[9] Hren, G. (2019). Numerical analysis of a wind turbine blade with different software. *Tehnicki Vjesnik*, *26*(4), 1017-1022. https://doi.org/10.17559/TV-20180615151600
[10] Yiğit, C. & Akman, E. (2021). Effect of two-dimensional profile optimization on vertical axis wind turbine power performance. *Tehnicki Vjesnik*, 28(1), 256-263. https://doi.org/10.17559/TV-20191112194157
[11] Shourangiz-Haghighi, A., Haghnegahdar, M. A., Wang, L., Mussetta, M., Kolios, A., & Lander, M. (2020). State of the Art in the Optimisation of Wind Turbine Performance Using CFD. *Archives of Computational Methods in Engineering*, *27*(2), 413-431. https://doi.org/10.1007/s11831-019-09316-0
[12] Karlsen, J. A. (2009). *Performance calculations for a model turbine.* Norwegian University of Science and Technology
[13] Ledoux, J., Riffo, S., Salomon, J., Ledoux, J., Riffo, S., Salomon, J., & Momentum, E. (2020). Analysis of the Blade Element Momentum Theory. *HAL Id : hal-02550763* https://doi.org/10.1137/20M133542X
[14] Spera, D. A. (1994). *Wind Turbine Technology: Fundamental Concepts of Wind Turbine Engineering*. ASME Press, New York
[15] Rocha, P. A. C., Rocha, H. H. B., Carneiro, F. O. M., da Silva, M. E. V., & de Andrade, C. F. (2016). A case study on the calibration of the k-ω SST (shear stress transport) turbulence model for small scale wind turbines designed with cambered and symmetrical airfoils. *Energy*, *97*, 144-150. https://doi.org/10.1016/j.energy.2015.12.081
[16] ElQatary, I. & Elhadidi, B. (2014). Comparison between OpenFOAM CFD & BEM theory for variable speed variable pitch HAWT, *ITM Web of Conferences*, *2*. https://doi.org/10.1051/itmconf/20140205001

Contact information:

Matej FIKE, PhD, Assistant Professor
(Corresponding author)
University of Maribor,
Faculty of Energy Technology,
Hočevarjev trg 1 8270 Krško, Slovenia
E-mail: matej.fike@um.si

Andrej PREDIN, PhD, Professor
University of Maribor,
Faculty of Energy Technology,
Hočevarjev trg 1 8270 Krško, Slovenia
E-mail: andrej.predin@um.si

Gorazd HREN, PhD, Associate Professor
University of Maribor,
Faculty of Energy Technology,
Hočevarjev trg 1 8270 Krško, Slovenia
E-mail: gorazd.hren@um.si

Marko PEZDEVŠEK, Teaching Assistant
University of Maribor,
Faculty of Energy Technology,
Hočevarjev trg 1 8270 Krško, Slovenia
E-mail: marko.pezdevsek@um.si